Robotics and Computer–Integrated Manufacturing 51 (2018) 73–84

Contents lists available at ScienceDirect

Robotics and Computer–Integrated Manufacturing

journal homepage: www.elsevier.com/locate/rcim

Full length Article

GA\SQP optimization for the dimensional synthesis of a delta mechanism based haptic device design

Guanyang Liu[a,b,*], Yinong Chen[b], Zheng Xie[b], Xuda Geng[b]

[a] State Key lab of Virtual Reality Technology and Systems, Beihang University, China
[b] School of Mechanical Engineering and Automation, Beihang University, China

ARTICLE INFO

Keywords:
GA, SQP
Optimization
DELTA mechanism
Haptic device

ABSTRACT

When designing a 3 DOF DELTA haptic device, a challenging problem is to optimize all the design variables to enable the DELTA mechanism to provide a desired cube workspace and perform well in haptic display. The designed haptic device should be able to exert required forces to a user in the whole workspace. Moreover, used as a haptic joystick to be installed in a dashboard, the outline envelope of the DELTA mechanism and driving motors are strictly restricted. The dimensional constraints on the designed device put forward much higher request on the dimension synthesis of DELTA mechanism to satisfy the requirements of output force and cube workspace simultaneously. The special constraints make the design of DELTA haptic joystick different from conventional DELTA robot design. In this paper, we solve the problem by using Genetic algorithms (GA) and sequential quadratic programming (SQP) and develop a DELTA haptic device. Through transforming the objectives and the constraints step by step, all proposed constraints are satisfied very well. For a haptic device, we explain the physical meaning of the condition number of the Jacobian matrix in force domain and use it as the criteria to evaluate the performance of a mechanism in haptic display. Experimental results and the prototype clearly demonstrate that the combination of SQP and GA (SQP uses the result of GA as the start point of all design variables) gives the optimal solution.

1. Introduction

The DELTA mechanism is a fully parallel mechanism and its mobile platform can only translate along the three Cartesian axes with respect to the base. Therefore, the DELTA robots, exhibiting high stiffness in nearly all configurations with a good dynamic performance, have been the most popular translational parallel manipulator [1–5].

High stiffness is also the reason why numerous haptic devices are developed based on the DELTA mechanism [6–11], such as Omega and Falcon. An impedance-typed haptic device that senses human hand motion and outputs feedback force/torque to the operator can be described as a special kind of robot. Working under the passive state and being manipulated by a user is the difference between a haptic device and a robot. For a DELTA robot design, the most challenging problem is the dimensional synthesis for a given workspace since the major drawback of a parallel mechanism is always its limited workspace.

This problem was addressed by Boudreau and Gosselin [12,13], and they proposed a genetic algorithm (GA) to obtain a workspace as close as to the prescribed one. Kosinka et al. [14] determined the variables of DELTA mechanism, where the prescribed workspace has been given in the form of a set of points. Snyman et al. [15] proposed an algorithm to design a 3-RPR manipulator requiring a two-dimensional reachable workspace. Laribi et al. [16,17] and Gallant et al. [18] proposed a novel genetic algorithm (GA) to deal with an optimal dimensional synthesis of DELTA robot for a prescribed workspace. Zi et al. [19,20] also proposed the method on design, analysis and control of a cable driven parallel robot WHCPM.

However, no research has been focused on the optimization and dimensional synthesis of DELTA haptic device as yet. Only considering the workspace is not enough to develop a DELTA haptic device. The constraints of required output force, confined outline envelope and cube workspace are coupled together.

Firstly, the workspace of the designed haptic device is required to be a cube, which can benefit operators in moving the handle along any direction conveniently and friendly. Secondly, the largest cube workspace has to be verified given a confined outline envelope since the designed haptic joystick will be installed into the interior of a console desk. Thirdly, the maximum feedback force has to be satisfied in the whole

* Corresponding author at: State Key lab of Virtual Reality Technology and Systems, Beihang University, China
E-mail address: gyliu@buaa.edu.cn (G. Liu).

https://doi.org/10.1016/j.rcim.2017.11.019
Received 6 June 2017; Received in revised form 7 October 2017; Accepted 28 November 2017
Available online 22 December 2017
0736-5845/

workspace with the selection of a driving system. The most important thing is that all these introduced constraints have to be satisfied at the same time.

Furthermore, the possible highest simulated stiffness is always preferred for a haptic device. Colgate [21] analyzed the factors affecting the Z-width of a haptic display and drawn the conclusion that the maximum achievable virtual stiffness is proportional to the sampling rate of a haptic loop with the inherent damping and virtual damping fixed. Controllers, control schemes and haptic rendering algorithms have received much attention [22–24] to minimize the sampling period of a haptic loop.

However, no author answers how to evaluate the impact of a mechanism on the sampling frequency of a haptic loop. In other words, the principle of dimensional synthesis to enable a designed haptic device to perform well in haptic display should be proposed and analyzed.

The condition number of the Jacobian matrix in velocity domain has always been used to design the mechanism of a robot to avoid singularity and keep the speed control smoothly. For a haptic device, the Jacobian matrix in force domain is the connection between output force and joint driving torques that computes the driving torques based on the required output force in any configuration. Although the Jacobian matrix in force domain and velocity domain have the same condition number, the condition number of Jacobian matrix should be given different physical meaning to be used as one criterion to evaluate the performance of a mechanism used as a haptic device.

Based on above introduction, if optimization algorithms are used to solve the above mentioned problem, the objectives should include the largest cube workspace with a restricted outline envelope, the desired maximum output force with a prescribed driving system, and the best achievable performance in haptic rendering. However, it is not a multi-objective optimization since all these objectives have priorities.

The ultimate objective is the performance of the DELTA mechanism in haptic display, and the initial constraint is the confined outline envelope. From the initial constraint, find the largest cube workspace and select a driving system. From the identified cube workspace and selected driving system, find the largest cube workspace meeting the requirement of maximum feedback force. Then, optimize all the design variables to enable the mechanism perform well in haptic display.

In fact, a multi-objective optimization problem is resolved into several single-objective optimizations based on their priorities and relationships, and the only given initial constraint is the restricted outline envelope. Based on the previous work [12–15], GA adapts to this typed optimization problem.

Genetic algorithms (GA) belong to the larger class of evolutionary algorithms (EA), which generate solutions to optimization problems using techniques inspired by natural evolution, such as inheritance, mutation, selection, and crossover. Genetic algorithms are independent on initial values of design variables and will not stick in local optima. This is the major reason why a GA algorithm is chosen for dimensional synthesis of the Delta mechanism used for designing a haptic device.

The sequential quadratic programming (SQP) with multiple initial points, the controlled random search (CRS), the differential evolution (DE), and the particle swarm optimization (PSO) are also widely used in the optimization and dimensional synthesis of serial or parallel mechanisms [25–27]. Especially, Lou [25] compared all these optimization methods in designing a DELTA robot, and SQP has been ranked highest in convergence rate based on experimental results.

In this paper, we use both SQP and GA to optimize the variables of the DELTA haptic device and compare the results. Based on analysis and repeated attempts, we combine the two methods that choose the result of GA as the start point of SQP. Experimental results demonstrate that the combination of SQP and GA gives the optimal solution, and the performance test of the prototype also validates the effectiveness of the proposed optimization scheme.

2. Optimal design problem formulation

The customer gives the confined outline envelope depending on the console design and the required maximum feedback force depending on human system engineering. What they need is a cube workspace as large as possible.

The optimization problem can be defined as searching a largest cube workspace based on the requirements of confined outline envelope and output force. The special working principle of an impedance typed haptic device determines the optimization is different from that of a conventional robot. Although the workspace is paid attention to both in the design of a haptic device and a robot, the capacity of exerting force in passive state rather than speed control in active state is focused on in the design of a haptic device.

The largest cube workspace has to be testified point by point to identify whether the required maximum output force can be reached in the whole workspace. Although the customer does not specify the driving system, outline dimension directly conditions the selection of a driving system. In other words, the maximum joint driving torque is also confined by outline dimension. Only after all constraints have been satisfied, all the design variables can be optimized to improve the performance of DELTA mechanism designed as a haptic device in haptic display; therefore, the best performance in haptic display is described as the final objective of the optimization.

Obviously, the constraints of confined outline envelope and maximum output force have the same priorities, and the objective of largest cube workspace has a higher priority than the mechanism performance in haptic display.

2.1. The initial constraint of confined outline envelope

Fig. 1 shows the 3D model and mechanism diagram of the being designed DELTA haptic device. From Fig. 2(a), the initial constraint of confined outline envelope on horizontal plane is $D \times W$, and no restriction in vertical direction. Fig. 2 depicts all the design variables of DELTA mechanism, R (the circum radius of the base), r (the circum radius of the mobile platform), L_A (the distance between points A_i and P_i), L_B (the distance between points B_i and P_i) and L_C (the width of the parallelogram mechanism).

Considering the outline envelope (Fig. 2(a) and (b)), the initial constraint can be computed:

$$L_C \sin 30° + \sqrt{3}(R + L_A) \le W$$

$$L_C \cos 30° \div 2 + (R + L_A) \times 3 \div 2 \le D$$

Based on the given value of $D \times W$, the relationship among L_A, L_C and R can be built. According to past experience, we firstly determine the variable L_C, and then the relationship between L_A and R can be identified. The reason why we give the value of variable L_C is that L_A and R together with L_B and r are the main four variables to affect the workspace of a DELTA mechanism.

2.3. The cube workspace

From Fig. 2(b), the tip point $O'(x, y, z)$ is the center of the upper moving platform, and the length of each mechanical chain can be calculated based on the geometry (Eq (1)):

$$\begin{aligned}&[(R-r+L_A\cos\theta_i)\cos\varphi_i - x]^2 \\ &+ [(R-r+L_A\cos\theta_i)\sin\varphi_i - y]^2 \\ &+ (-L_A\sin\theta_i + z)^2 = L_B^2\end{aligned} \tag{1}$$

After calculation, Eq. (2) with Eqs. (3)–(5) can be identified:

$$A_i \cos\theta_i + B_i \sin\theta_i + C_i = 0 \tag{2}$$

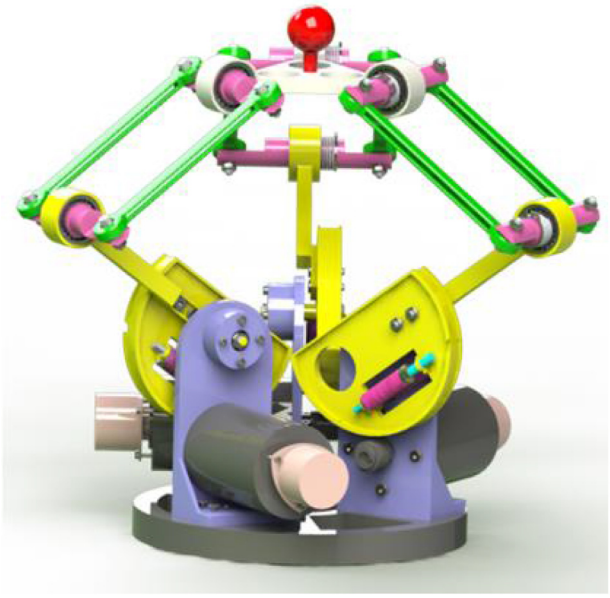

(a): 3D model of the designed DELTA haptic device

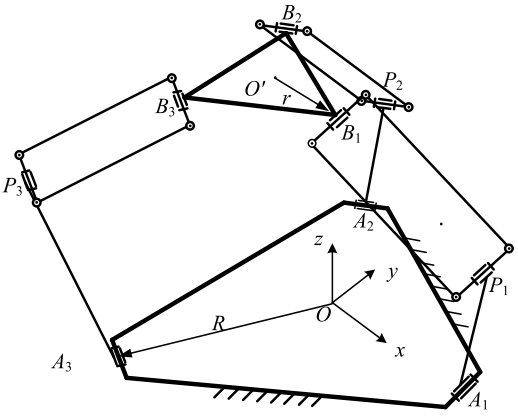

(b): mechanism diagram of the DELTA mechanism

Fig. 1. 3D model and diagram of the DELTA haptic device.

$$A_i = 2L_A[(R-r)-x\cos\varphi_i - y\sin\varphi_i]\cos\theta_i \tag{3}$$

$$B_i = 2L_A z\sin\theta_i \tag{4}$$

$$C_i = L_A^2 - L_B^2 + (R-r)^2 + x^2 + y^2 + z^2 - 2x(R-r)\cos\varphi_i - 2y(R-r)\sin\varphi_i \tag{5}$$

Based on the following trigonometric function,

$$A_i\cos\theta_i + B_i\sin\theta_i \le \sqrt{A_i^2 + B_i^2}$$

Eq. (6) is obtained:

$$[x^2 + y^2 + z^2 - 2(R-r)(x\cos\varphi_i + y\sin\varphi_i) + L_A^2 - L_B^2 + (R-r)^2] - 4L_A^2[(x\cos\varphi_i + y\sin\varphi_i - (R-r))^2 + z^2] \le 0 \tag{6}$$

Eq. (6) is the condition to identify whether a target point can be reached by the center $O'(x, y, z)$ of the upper mobile platform. From

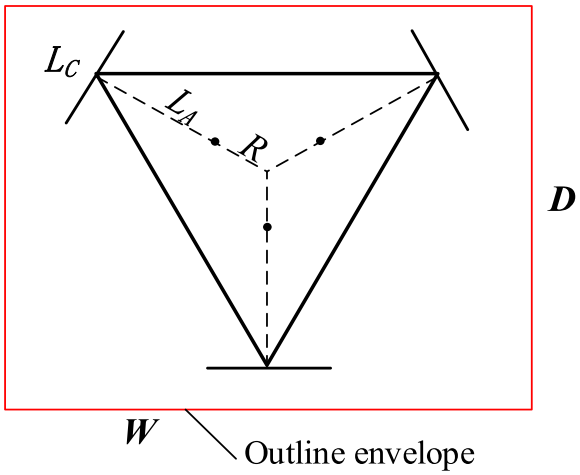

(a): the moving platform and the base from top view

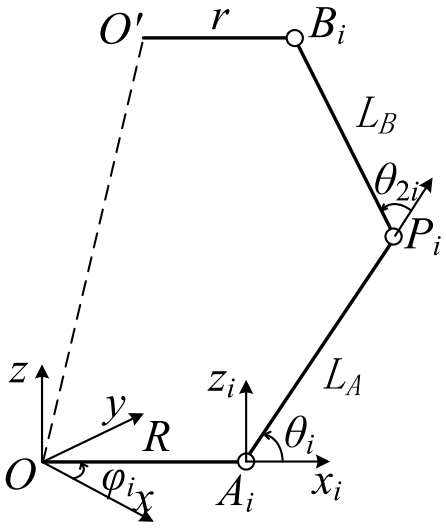

(b): the moving platform, the base and a chain from main view

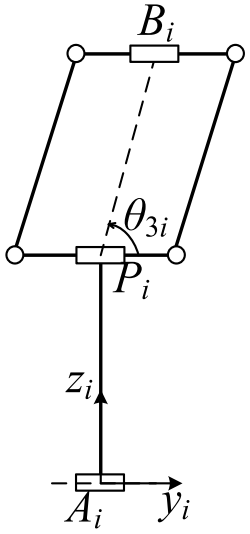

(c): a chain from side view

Fig. 2. All the design variables of DELTA mechanism.

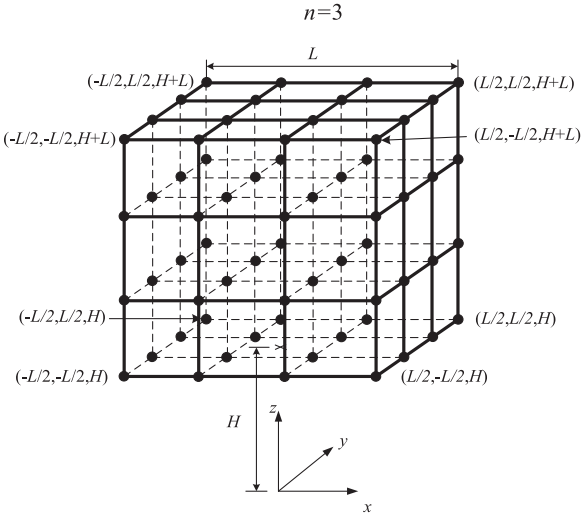

Fig. 3. All the sub-cubes of the cube workspace when n = 3.

Eq. (7), we define a function $h(i)$ for each mechanical chain of the DELTA mechanism as follows:

$$h(i) = \left[x^2 + y^2 + z^2 - 2(R-r)(x\cos\varphi_i + y\sin\varphi_i) + L_A^2 - L_B^2 + (R-r)^2\right] - 4L_A^2\left[(x\cos\varphi_i + y\sin\varphi_i - (R-r))^2 + z^2\right] \quad (i = 1,2,3) \tag{7}$$

If $h(i) \le 0 (i = 1,2,3)$, then the current center $O'(x, y, z)$ of the moving platform belongs to the workspace of the Delta mechanism. Otherwise, the current position cannot be reached by the center of the upper mobile platform. In order to identify the maximum cube workspace, from Fig. 3, a cube is divided into n^3 same cube cells along the x-axis, y-axis and z-axis. If all eight vertices of a cube cell meet the above mentioned condition (Eq. (7)), this cube unit is definitely contained by the whole workspace of the Delta mechanism.

The dimension of a cube cell depends on the required resolution of the designed haptic device. Smaller the cube cell is, higher the position resolution is. From Fig. 3, if all the $(n+1)^3$ vertices of all the n^3 unit cells meet the requirement (Eq. (7)), all the n^3 cube cells are in the workspace of the being designed Delta mechanism. Therefore, the maximum value of n and the dimension of a cube cell describe the maximum cube workspace of a DELTA mechanism.

2.4. The required output force and driving torque constraints

As the driving system is selected according to the dimensional constraints, the mechanical structure has to enable the maximum joint driving torque 0.8 Nm to satisfy the required maximum output force 3 N at any point of the whole cube workspace. Eq. (8) depicts the relationship between the output force and the driving torque:

$$\begin{aligned} &\boldsymbol{\tau} = J_F\mathbf{F} \\ &\boldsymbol{\tau} = \left[\tau_1\tau_2 \quad \tau_3\right]^T \\ &\mathbf{F} = \left[F_xF_yF_z\right]^T \end{aligned} \tag{8}$$

Where, J_F is the Jacobian matrix in force domain, J is the Jacobian matrix in velocity domain, and $J_F = (J^T)^{-1}$. In order to guarantee the magnitude of the output force $\mathbf{F}$ reaches the specific maximum value at any point of the cube workspace, the maximum joint driving torque τ_{max} is calculated (Eq. (9)):

$$\tau_{max} \ge \max_{i=1}^{3}(\max_{\forall\|\mathbf{F}\|}|\tau_i|) \tag{9}$$

Where, τ_i is the driving torque of the i joint and $\forall\|\mathbf{F}\|$ is the output force in arbitrary direction. $\max_{\forall\|\mathbf{F}\|}|\tau_i| = \max_{\forall\|\mathbf{F}\|}|j_{i1}F_x + j_{i2}F_y + j_{i3}F_z| (i = 1,2,3)$ j_{ij} is the element of the Jacobian matrix J_F. Define constraint $\|\mathbf{F}\| = \hat{F}$, and define Lagrange function (Eq. (10)),

$$L = j_{i1}F_x + j_{i2}F_y + j_{i3}F_z \quad + \lambda(F_x^2 + F_y^2 + F_z^2 - \hat{F}^2) \tag{10}$$

Each force component can be calculated (Eq. (11)):

$$F_k = j_{i1}\hat{F}/\sqrt{j_{i1}^2 + j_{i2}^2 + j_{i3}^2} \quad k = x, y, z \tag{11}$$

Then, the required maximum driving torque at any point in the whole workspace is identified (Eq. (12)):

$$\tau_{max} = \hat{F}\max_{i=1}^{3}\sqrt{j_{i1}^2 + j_{i2}^2 + j_{i3}^2} \tag{12}$$

2.5. The objective function

To develop a robot, the condition number of Jacobian matrix in velocity domain is usually used to evaluate the performance of a mechanism in speed control. The speed change of the end-effector should not result in a violent variation of the driving motors to avoid singularity and implement smooth speed control.

For haptic display, decreasing the variation of required motor driving torques between two sampling periods (1 ms) of a haptic loop is greatly beneficial to performing well and achieving stability [28]. The principle of developing haptic rendering algorithms can also be used for reference to designing a mechanism used as a haptic device [21]. Eq. (13) builds the relationship between the output force and joint driving torques.

$$\mathbf{F} = \mathbf{J}_\mathbf{F}^{-1}\boldsymbol{\tau} \tag{13}$$

Where, $\mathbf{J}_\mathbf{F}^{-1}$ is the inverse of the Jacobian matrix in the force domain. $\mathbf{J}_\mathbf{F}^{-1}$ should satisfy the objective that the variation of driving torque is the minimum when the required output force $\mathbf{F}$ varies from 0 to $\mathbf{F}_{max}$ (the maximum output force). It is expected that a large change of $\mathbf{F}$ results in a small change of τ at a sampling period. The requirement is similar to the stabilization principle of haptic rendering algorithms. $\mathbf{J}_\mathbf{F}^{-1}$ is the evaluation criterion in force domain of the performance of a mechanism used as a haptic device, and the condition of the matrix $\mathbf{J}_\mathbf{F}^{-1}$ should be as small as possible to enable the mechanism to perform well in haptic display. Eqs. (14) and (15) are used to calculate the matrix condition number.

$$k(\mathbf{J}_\mathbf{F}^{-1}) = k(\mathbf{J}) \tag{14}$$

$$k(\mathbf{J}) = \|\mathbf{J}\| \cdot \left\|\mathbf{J}^{-1}\right\| \tag{15}$$

Where, $\mathbf{J}$ is the Jacobian matrix in the velocity domain. It is very interesting that the same condition number of Jacobian matrix in force domain and velocity domain represents the same criterion to evaluate a mechanism for robot design and haptic device design. The essence of a mechanism decides the phenomenon that the relationship between the speed of end-effector and the velocity of driving joints has the same change rule with the relationship between the output force of end-effector and joint driving torques. Whether used as a robot or a haptic device, the criterion to evaluate a mechanism is the same. From Eq. (16), the parameter η is proposed to evaluate the performance of a haptic mechanism.

$$\eta = \min(max k(\mathbf{J}_\mathbf{F}^{-1})|_{P_i}); (i = 1, 2...) \tag{16}$$

According to the cask theory, the minimum η is the final objective function of the DELTA mechanism optimization.

3. Optimization algorithm

The initial constraint is the confined outline envelope of the DELTA mechanism, and the final objective is to obtain the optimal values of the design variables to enable the mechanism to perform well as a haptic device. Moreover, the relationship of the required maximum output force and the selected driving system have to be satisfied.

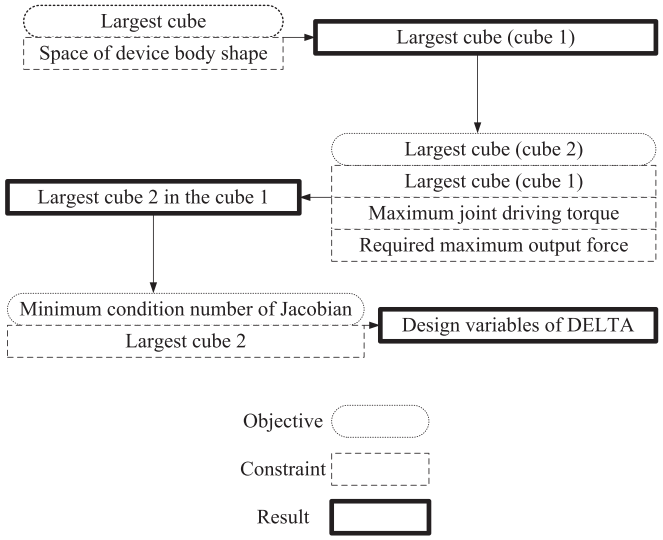

Fig. 4. The procedure of the optimization step by step.

The optimization seems like a multi-objective and multi-constraint problem, however, it can be divided into three single-objective and multi-constraint optimizations in Fig. 4. First of all, we have to identify the largest cube workspace while only the constraint of the confined outline envelope is satisfied. For this step, the confined outline envelope is the only constraint, and the largest cube workspace is the objective.

For the second step, the whole cube workspace obtained from step 1 has to be traversed point by point to identify whether the relationship of maximum output force and joint driving torques can be met. The optimization result of step 2 can illustrate that none, a part or the whole of the cube workspace obtained at step 1 can meet the constraint of maximum output force and joint driving torques.

Only when a cube workspace can be found at step 2, the design variables of the DELTA mechanism need to be optimized to improve its performance in haptic display; otherwise, no DELTA mechanism based haptic joystick can satisfy all the constraints proposed by the customer.

The proposed optimization methodology combines three steps of single-objective feasibility analysis and optimization, and the reached objective at the last step becomes the constraint at the current step. It can be seen from Fig. 4 that the results of the first two steps draw a conclusion that whether the design work can be implemented.

The procedure of the optimization is divided into three steps.

a) The first step

Optimization to obtain the largest cube W for a given constraint of confined outline envelope C
Outcome of the optimization: the largest cube W and the relationship among all four design variables

b) The second step

Optimization to obtain the largest cube W_d ($W_d \in W$) to satisfy the constraints of the output force and the driving system
Outcome of the optimization: the largest cube W_d and the relationship among all the four design variables

c) The third step

Optimal dimensional synthesis of the Delta mechanism to have the best performance as a haptic device
Outcome of optimization: all the four design variables established to obtain the minimum η.

4. Optimization results and discussion

The goal is to obtain the optimal design variables of the DELTA mechanism to design a haptic device with given constraints. The constraints are listed as below:

- For the mechanism configuration, the restriction on horizontal plane is smaller than 220×270 mm, and no restriction in vertical direction
- The required maximum output force is 3 N
- The maximum joint driving torque is 0.8 N·m

Considering the engineering application that the device has to be assembled in a console desk, we define the variable $R = 40$ mm. According to the relationship between L_A and R, we define the variable L_A=82 mm to obtain the possible maximum workspace.

As above introduced, the whole process of the optimization is divided into three steps, Table 1 depicts the constraints, design variables and objective for each step. The GATOOL of MATLAB is used for the implementation of the optimization.

In Table 1, the side length of a cube workspace is $2L$, and the initial (original) distance between the upper moving platform and the base is H, which are shown in Fig. 3. After step 2, the maximum cube workspace of the DELTA mechanism satisfying the constraints of confined outline envelope and the maximum output force can be obtained. For the final step, all the design variables are optimized to enable the mechanism to perform well in haptic display.

4.1. GA based method

Firstly, all the parameters of the GA optimization for each step are listed in Table 2, and the bounds lower and upper of each design variable for step 1 are listed in Table 3. We repeat the GA optimization with the same bounds of each variable four times. Table 4 displays all the results which only have very small difference. We change the bounds of each design variable (Table 5) and repeat the optimization. The results (Table 6) show that larger cube workspace ($67.16 > 64.25$) can be obtained, which demonstrates that the dimension of the achieved cube workspace is very sensitive to the bounds of each variable in the first step of the optimization.

Table 7. illustrates the bounds of each design variable for the second step of the optimization. The bounds of L_B are changed step by step since the final result is found to be very sensitive to the bounds of variable L_B at the first step.

From Table 7, the results also show that the design variable L_B influences the original distance H between the upper moving platform and the base of DELTA mechanism when the handle is kept to stay at the origin of the whole cube workspace. However, it nearly does not affect the size of the cube workspace required at step 2. Although a larger cube workspace can be found by enlarging the length of variable L_B at step 1, no larger cube workspace meeting the maximum output force requirement can be obtained by repeating the same operation at step 2.

Table 8 illustrates that the bounds selection of design variables in the GA optimization influences the final result for step 3. Therefore, when using GA optimization, the bounds of each design variable should be reasonably set and adjusted to find the optimal results.

Figs. 5 and 6 depict the GA optimization results step by step. In Fig. 5, the red cube is the maximum cube workspace with a side length of $2L$ to meet the constraint of confined mechanism body space. From Fig. 6, the red cube with a side length of $2L$ can meet the constraints of confined outline envelope and maximum output force simultaneously. The discrete red points between the cube space of Fig. 6 and the cube space of Fig. 5 do not satisfy the constraint of maximum output force even if they can meet the requirement of confined outline envelope. Therefore, the yellow cube in Fig. 6 is the expected largest cube workspace for the mechanism used as a haptic joystick.

Table 1
The constraints, variables and objectives for each step of the optimizations.

Step	Constraints	Variables	Objective
1	$R + L_A \le 122,\ R = 40,\ L_A = 82$	$L_A, L_B, R\ r, L, H$	$F(X) = \max L;\ X = (L_A, L_B, R, r, H, L)$
2	$R + L_A \le 122,\ R = 40,\ L_A = 82\ \tau_{i\max} > \hat{F}\sqrt{j_{i1}^2 + j_{i2}^2 + j_{i3}^2}$	$L_A, L_B, R\ r, L, H$	$F(X) = \max L;\ X = (L_A, L_B, R, r, H, L)$
3	L Obtained at step 2	$L_A, L_B, R\ r, H$	$F(X) = \min(maxk(\mathbf{J}_\mathbf{F}^{-1})\|_{P_i})\ (i = 1, 2...)$

Table 2
The parameters of the GA by using GATOOL of MATLAB.

Step	1	2	3
Population Size	100	220	220
Number of Variables	6	6	4
Crossover Fraction	0.8	0.8	0.8
Migration Fraction	0.2	0.2	0.2
Maximum Generations	100	100	100

Table 3
Bounds lower and upper of each design variable for step 1 of GA optimization.

Design variables	Value
L_A, L_B, R, r, H, L Bounds lower	[82,40,40,20,40,0]
L_A, L_B, R, r, H, L Bounds upper	[82,130,40,45,100,100]

Table 4
The results of repeating the GA optimization with the same bounds of each variable for step 1.

Time No.	1	2	3	4
L_A	82	82	82	82
L_B	129.625	129.351	129.862	129.992
R	40	40	40	40
r	40.545	39.417	40.92	41.13
H	47.5	47.5	48	48
L	64.25	64.25	64.25	64.2

Table 5
Bounds lower and upper of each variable for GA optimization.

Design variables	Value
L_A, L_B, R, r, H, L Bounds lower	[82,40,40,20,40,0]
L_A, L_B, R, r, H, L Bounds upper	[82,170,40,45,100,100]

Table 6
The results of repeating the GA optimization when changing the bounds of L_B for step 1.

L_A	82
L_B	163.023
R	40
r	39.717
H	81.022
L	67.16

Table 7
The design variables and optimization results step 2.

L_A, L_B, R, r, H, L Bounds lower	L_A, L_B, R, r, H, L Bounds upper	L_A, L_B, R, r, H, L Results
[82,100,40,20,40,0]	[82,120,40,40,60,75]	82, 116.5, 40, 39.2, 54.0,37.7
[82,100,40,20,40,0]	[82,130,40,40,60,75]	82, 120.0, 40, 40.0, 57.1,37.5
[80,100,40,20,40,0]	[82,170,40,40,60,75]	82, 122.6, 40, 37.6, 60.0,37.6

Table 8
The design variables and optimization results for step 3.

L_B, r, H Bounds lower	L_B, r, H Bounds upper	$L_B, r, H, F(X)$ Results
[80,30,50]	[140,40,70]	119, 30, 63.098, 6.570
[100,30,40]	[130,40,65]	114.0, 30, 58.737, **6.136**

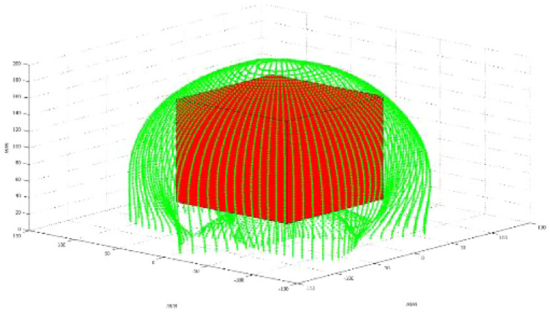

Fig. 5. 3D output of the largest cube in workspace envelope.

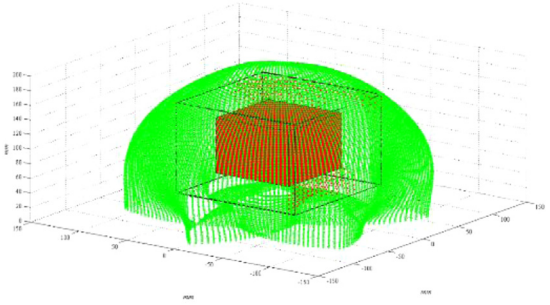

Fig. 6. 3D output of the largest cube in the cube workspace obtained at the second step.

4.2. SQP method

SQP is also implemented to solve the design and optimization problem proposed in this paper to be compared with GA. We use MATLAB Optimization Tool, select function FMINCON and SQP algorithm. However, SQP is different from GA that the selection of the start point greatly influences the final optimization result. From Table 9, unsuitable start point leads to divergence. By using SQP, the optimization result of step 1 is very close to that of GA. Table 9 illustrates the results of SQP optimization for step 1.

However, for the second and third step of the optimization, SQP can find better solution of L ($39.2 > 37.3$) and $F(X)$ ($6.009 < 6.136$) than GA in Tables 10 and 11. Although the selection of start point leads to divergence sometimes, a conclusion can also be drawn that SQP can find better optimization results than GA while all variables have the same bounds.

4.3. Discussion on GA and SQP

The above introduced experimental results illustrate that both GA and SQP can solve the problem of DELTA mechanism based haptic device design. For GA, its advantage is that no start point is required and wrong selection of start point for SQP will lead to divergence. Therefore, the optimization result of SQP depends on the selection of start point.

Although SQP can obtain better solution than GA, the SQP optimization does not converge with unsuitable start points. GA optimization does not need start point; therefore, we use the result of GA optimization as the start point of SQP optimization. Table 12 shows that selecting the GA optimization result as the start point of SQP optimization can

Table 9
The variables and optimization results by using SQP for step 1.

Start point	L_A, L_B, R, r, H, L Bounds lower	L_A, L_B, R, r, H, L Bounds upper	L_A, L_B, R, r, H, L Results
[80,100,40, 40,50,40]	[50,0,20, 30,40,35]	[90,130,80, 50,60,200]	82,130,40, 40,58,*64.2*
[80,100,40, 40,50,40]	[50,0,20, 30,40,35]	[90,140,80, 50,60,200]	82,140,40, 40,48,*65.2*
[80,100,40, 40,50,40]	[50,0,20, 30,40,35]	[90,150,80, 50,60,200]	82,142,40, 40,60,*65.4*
[80,100,40, 40,50,40]	[80,100,40, 20,40,30]	[82,130,40, 40,60,150]	82,130,40, 40,48,*64.4*
[80,100,40, 40,50,**41**]	[80,0,20, 30,40,30]	[82,130,40, 40,60,150]	*No results*
[80,100,40, 40,50,40]	[80,100,40, 40,40,30]	[82,130,40, 40,60,150]	82,130,40, 40,48,*64.4*
[80,100,**30**, 40,50,40]	[80,100,40, 30,40,30]	[82,130,40, 40,60,150]	*No results*
[80,100,40, 40,50,40]	[80,100,40, 40,40,30]	[82,130,40, 40,60,150]	82,130,40, 40,48,**64.4**
[80,100,**30**, 40,50,40]	[80,100,40, 30,40,30]	[82,130,40, 40,60,150]	*No results*

Table 10
The variables and optimization results by using SQP for step 2.

Start point	L_A, L_B, R, r, H, L Bounds lower	L_A, L_B, R, r, H, L Bounds upper	L_A, L_B, R, r, H, L Results
[82,100,40, 40,50,40]	[82,0,40, 10,40,35]	[82,130,40, 50,60,100]	82,122.8,40, 19.6,60,*39.2*
[82,100,30, 40,50,40]	[82,0,40, 20,40,35]	[82,130,40, 50,60,100]	82,122.4,40, 20,59.7,*39.2*
[82,100,30, 40,50,40]	[82,0,40, 30,40,35]	[82,130,40, 50,60,100]	82,112.5,40, 30,50.7,*38.4*
[82,100,30, 40,50,40]	[82,0,40, 30,40,35]	[82,140,40, 50,60,100]	82,112.5,40, 30,50.7,*38.4*
[82,100,40, 40,50,40]	[82,0,40, 30,40,35]	[82,130,40, 50,60,100]	*No results*

Table 11
The variables and optimization results by using SQP for final step.

Start point	L_B, r, H Bounds lower	L_B, r, H Bounds upper	L_B, r, H, $F(X)$ Results
[100,30,60]	[0,30,40]	[130,50,150]	112.1,30,57.1,*6.009*
[100,30,60]	[0,30,40]	[140,50,150]	112.0,30,57.1,*6.009*

Table 12
The variables and optimization results by using GA and GA+SQP.

Start point	L_B, r, H Bounds lower	L_B, r, H Bounds upper	L_B, r, H, $F(X)$ Results
GA No	[80 30 50]	[140 40 70]	119, 30, 63.098, *6.570*
GA+SQP [119, 30, 63.098] Obtained from GA	[0,30,40]	[130,50,150]	112.1, 30, 57.1, *6.009*
GA No	[100,30,40]	[130,40,65]	113.989, 30, 58.737, *6.136*
GA+SQP [113.989, 30, 58.737] Obtained from GA	[100,30,40]	[130,40,65]	112.079, 30, 57.112, *6.009*

greatly benefit us in finding better solutions $F(X)$ ($6.009 < 6.136$). Even if the start points are different (Table 12), the SQP can find the same optimal solution $F(X)$ (6.009). Using GA optimization to find the start point of SQP optimization should be an effective way to enable the SQP optimization more useful and efficient.

5. Demonstration of the proposed optimization by using the designed haptic device

Fig. 7 shows the designed DELTA haptic joystick. By using the three-coordinates measuring machine, the side length of the cube workspace of the designed device is measured to be larger than 70 mm. We develop a mechanical structure (Fig. 8) to testify the cube workspace of the designed haptic device, and the side length of the square hole (Fig. 8) is 70 mm. During the experiment, the handle can be manipulated to move in the square hole freely, and all the eight vertices and six faces of the square hole can be reached without any barrier. The experimental result illustrates that the DELTA mechanism can achieve the optimal cube workspace by using the proposed optimization method.

As above introduced, a haptic device is usually developed for virtual reality or remote robot control. When a user manipulates the designed haptic joystick to enter a virtual environment or control a slave robot,

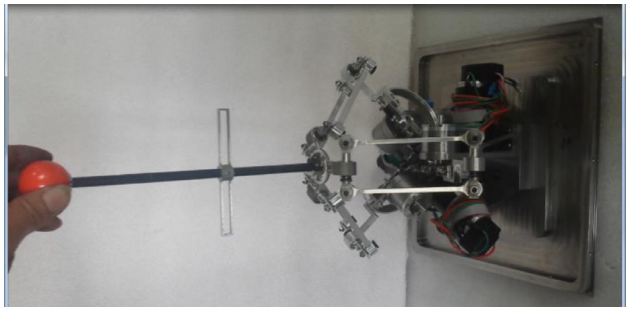

Fig. 7. The designed prototype of the 3DOF DELTA mechanism based haptic joystick.

the user should only feel feedback forces generated by rendering algorithms, which means the gravity of all moving parts cannot influence the hand motion and hand feeling of a user. The hand feeling of gravity restricts and weakens the transparency of the haptic device as an interface between a user and virtual environments or remote environments. Therefore, the gravity of all moving parts has to be compensated and balanced. Gravity compensation should enable the handle to stay at any position of its whole cube workspace without being touched by a user before the operating resistance and contact force being rendered.

5.1. Gravity compensation

All parts of the designed haptic device are symmetrical and homogeneous, and the mass of each part is decided based on the constraint of gross weight. From Fig. 9, the mass of upper moving platform O^1 is m_1, the mass of active link A_iP_i is m_2, the mass of passive link B_iP_i is m_3.

The mass of upper moving platform and passive link P_iB_i can be equivalent to the joint B_i, the equivalent gravity $\mathbf{G}_B$ is computed as follow,

$$\mathbf{G}_B = [0, 0, (\frac{1}{3}m_1 + \frac{1}{2}m_3)g] \tag{17}$$

The mass of active link A_iP_i and passive link B_iP_i can be equivalent to the joint P_i, the equivalent gravity $\mathbf{G}_P$ is computed as follow,

$$\mathbf{G}_P = [0, 0, (\frac{1}{2}m_2 + \frac{1}{2}m_3)g] \tag{18}$$

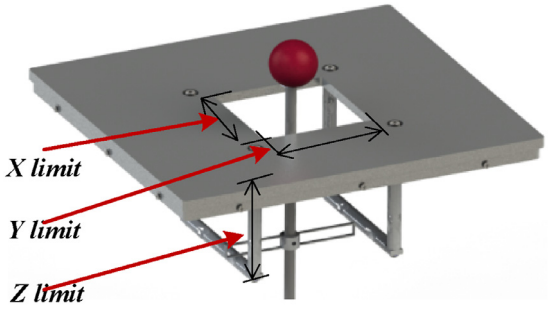

(a)

(b)

Fig. 8. The mechanical structure used to depict the cube workspace.

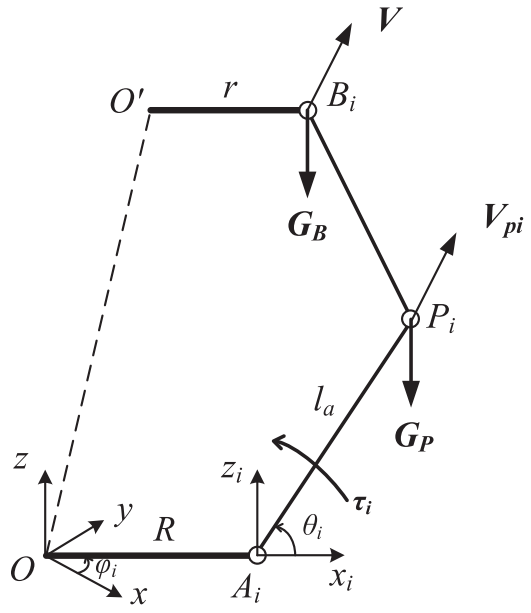

Fig. 9. The diagram of a mechanical chain of the designed DELTA mechanism.

We define the joint driving torque $\boldsymbol{\tau} = [\tau_1, \tau_2, \tau_3]$, based on the principle of virtual work, the input power equals the output power,

$$\boldsymbol{\tau}\dot{\boldsymbol{\theta}}^T = 3\mathbf{G}_B\mathbf{V}^{\mathrm{T}} + \mathbf{G}_P(\mathbf{V}_{P1}^{\mathrm{T}} + \mathbf{V}_{P2}^{\mathrm{T}} + \mathbf{V}_{P3}^{\mathrm{T}}) \tag{19}$$

Where, the velocity of the moving platform is $\mathbf{V} = (\dot{x}, \dot{y}, \dot{z})$, the angular velocity of each driving joint is $\dot{\boldsymbol{\theta}} = (\omega_1, \omega_2, \omega_3)$, the translational velocity of joint P_i is $\mathbf{V_{Pi}}(i = 1, 2, 3)$.

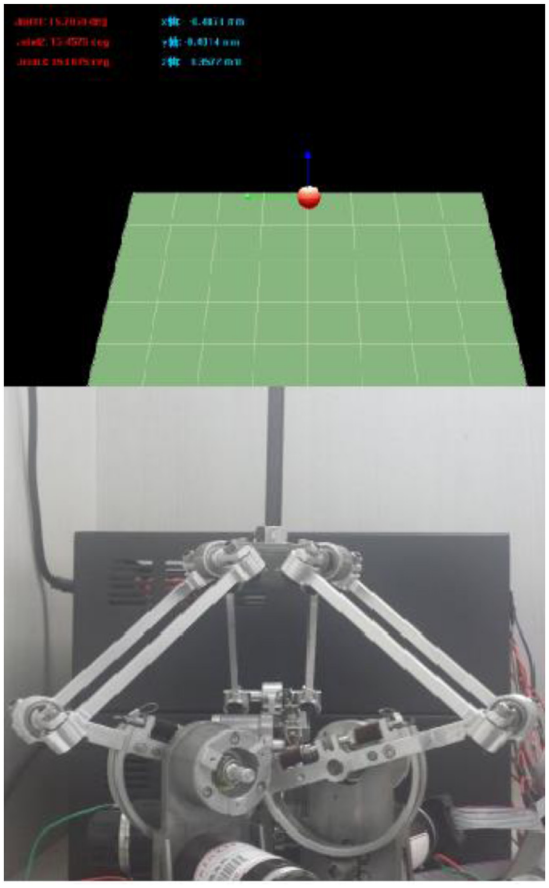

Fig. 10. Testing handle of the DELTA mechanism based haptic device can stay at its original center position without being touched.

We define that the unit vector along the axis y_i is $\mathbf{n}_i(i = 1, 2, 3)$, the following equation (Eq. (20)) can be obtained,

$$\begin{bmatrix} \mathbf{V_{P1}} \\ \mathbf{V_{P2}} \\ \mathbf{V_{P3}} \end{bmatrix} = \begin{bmatrix} (\mathbf{n}_1 \times \mathbf{A_1P_1})\omega_1 \\ (\mathbf{n}_2 \times \mathbf{A_1P_2})\omega_2 \\ (\mathbf{n}_3 \times \mathbf{A_1P_3})\omega_3 \end{bmatrix} \tag{20}$$

$$J \cdot \mathbf{V} = J_{\theta} \cdot \dot{\boldsymbol{\theta}} \tag{21}$$

Where, J is the Jacobi matrix in the velocity domain, and J_{θ} is the inverse of Jacobi matrix. Based on the Eqs. (20) and (21), the following result can be obtained and simplified,

$$\boldsymbol{\tau} = 3\mathbf{G}_B J^{-1} + \mathbf{G}_P \begin{bmatrix} \mathbf{n}_1 \times \mathbf{A_1P_1} \\ \mathbf{n}_2 \times \mathbf{A_1P_2} \\ \mathbf{n}_3 \times \mathbf{A_1P_3} \end{bmatrix} \tag{22}$$

Based on the Eq. (22), the required driving torque of each joint to balance the gravity can be identified at any configuration in real time. Through compensating the gravity, users will only feel rendered feedback force without any other weight.

Fig. 10 shows the handle staying at its original position without being touched by using the proposed gravity compensation method. The red ball in the virtual environment is the avatar of the tip of the device handle. To keep the handle staying at the origin, the computed output torques of the three motors mounted in the device are 16.18mN·m, 16.28mN·m and 16.34mN·m respectively.

Fig. 11 shows the handle that is moved to a random position in its cube workspace, and the current position of the handle is 1.5243 mm, 17.6991 mm and 33.3409 mm. The handle can stay at the current position without being touched, and the computed output torques of the three motors are 15.62 mN·m, 13.45 mN·m and 18.76 mN·m respectively.

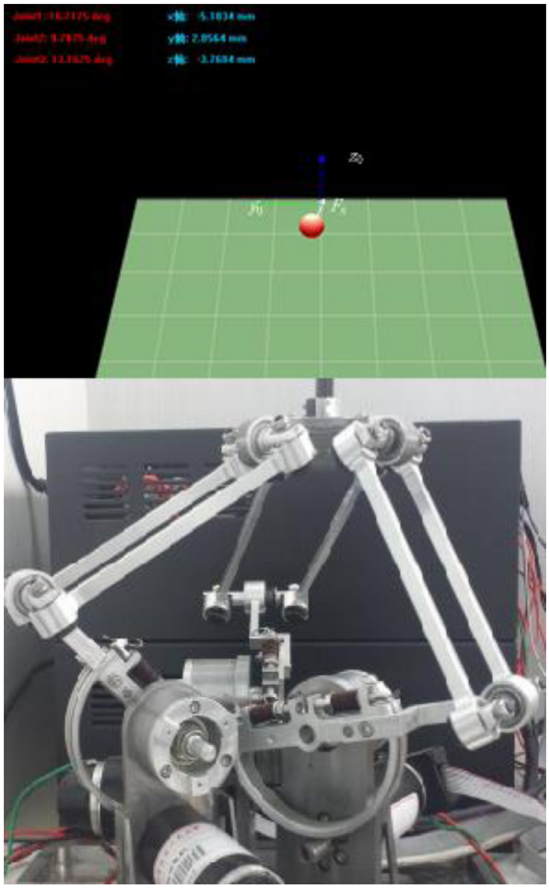

Fig. 11. Testing handle of the DELTA mechanism based haptic device can stay at a position of its workspace without being touched, and the effect is implemented by using gravity compensation.

Experimental results clearly show that the handle can stay at any position in its workspace without being touched, and the gravity compensation is effective to enable users to move the handle with zero resistance.

5.2. Rendered operating resistance

When a user manipulates the designed haptic joystick, he should feel operating resistance to maintain a user-friendly manipulation. The model for resistance rendering is shown in Fig. 12.

Based on Fig. 12, the force model to compute the operating resistance is provided as follow,

$$\mathbf{F_k}=\begin{cases} 0 & 0<d<r_0 \\ k\times(d-r_0)\times\mathbf{e_{OO'}}-b\mathbf{v} & r_0<d<r_1 \\ k\times(r_1-r_0)\times\mathbf{e_{OO'}}-b\mathbf{v} & r_1<d \end{cases} \tag{23}$$

Where, $\mathbf{F_k}$ is the feedback force, k is the spring stiffness, b is the damping coefficient, r_0 is the radius of a dead zone, r_1 is the switch of constant force and spring force, d is the distance from the current position to the origin, $\mathbf{e_{OO'}}$ is the unit vector from the current position to the origin, $\mathbf{v}$ is the current translational velocity of the handle.

From Eq. (23), the spring-damping model and constant force are used to render the operating resistance to a user. The constant force equals the value of spring-damping model at switching point r_1 (Fig. 12). A very small dead zone with no output force is set up to guarantee the home function to keep the handle staying stably at the origin. A damping force is always required in haptic display to keep the haptic device work stably.

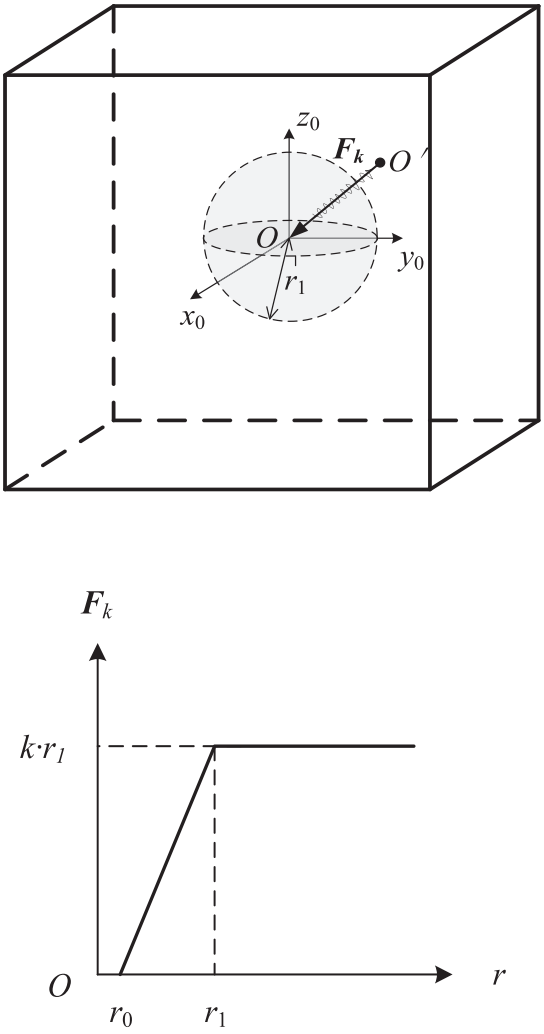

Fig. 12. The diagram to depict the force model to render resistance.

A specially designed instrument is used to measure the operating resistance provided by the designed haptic joystick and validate the proposed force model. From Fig. 13, an ATI NANO 17 sensor is mounted between the handle of the instrument and the shaft of the designed haptic joystick, and the react force between the device and the operator can be measured. An experiment is developed that a user manipulates the handle to move it from the origin to the boundary of the cube workspace. During the whole process of manipulation, the output force of the device is measured and recorded by using the specially designed instrument.

Figs. 14 and 15 show the measured forces when a user manipulates the haptic device to move its handle to a vertex of the whole cube workspace. Fig. 14 shows the measured feedback force that the radius of dead zone is 1.5 mm, the radius of switch point is 10 mm, the spring stiffness is 0.4 N/mm, and the damping coefficient is 500 N·s/m. Fig. 15 shows the measured feedback force that the radius of dead zone is 1.5 mm, the radius of switch point is 5 mm, the spring stiffness is 0.8 N/mm, and the damping coefficient is 500 N·s/m.

Users can feel very smooth and stable feedback force with no sudden change of output force and no oscillation. Users can also move the handle to the eight vertices of the cube workspace (Fig. 8), and the feedback forces all reach 3 N. The experimental results testify that the constraint of required maximum output force can be satisfied and the result of GA/SQP optimization is correct.

As a haptic joystick used for HCI or HMI, it should have the home function that the handle can automatically move back to the origin from

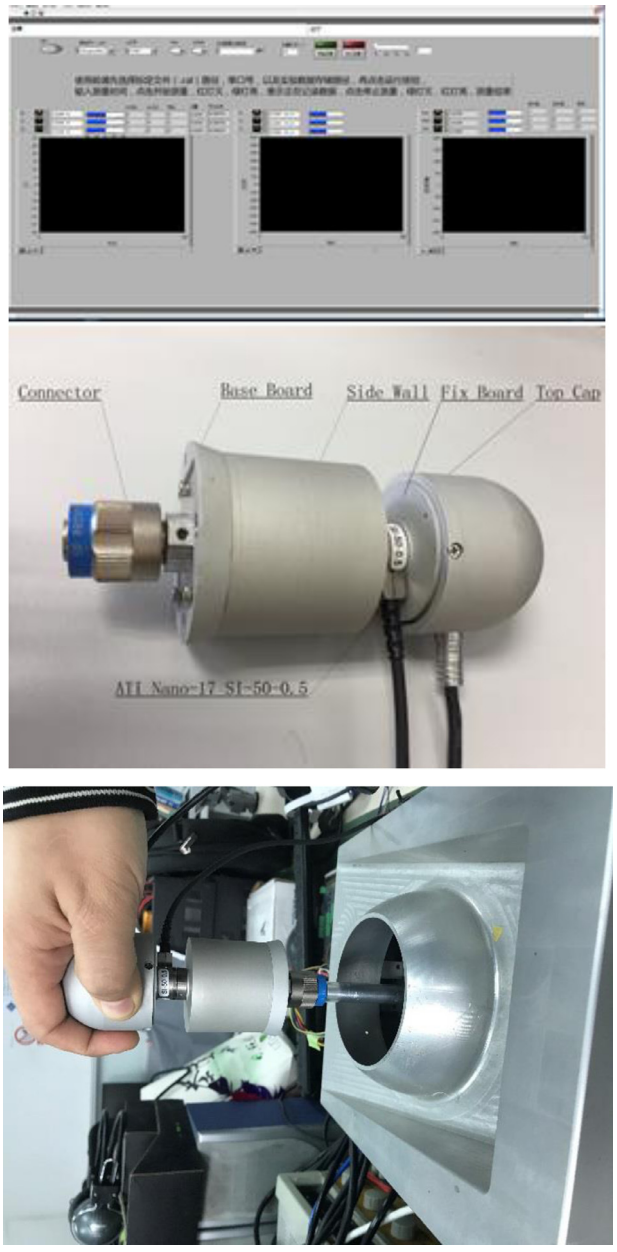

Fig. 13. A designed instrument to measure the operating resistance rendered by the proposed force model.

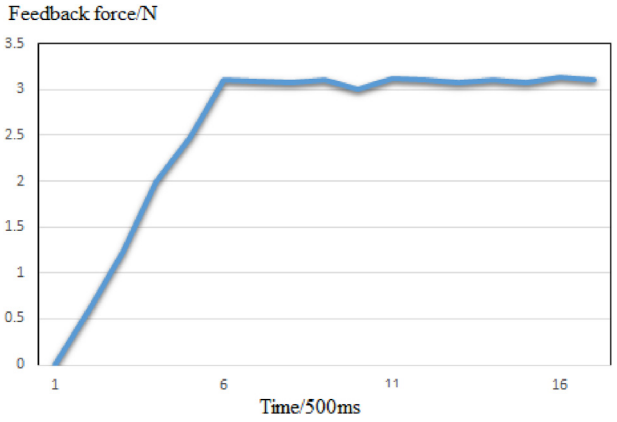

Fig. 14. The measured operating resistance by using the instrument with different setting of force model variables.

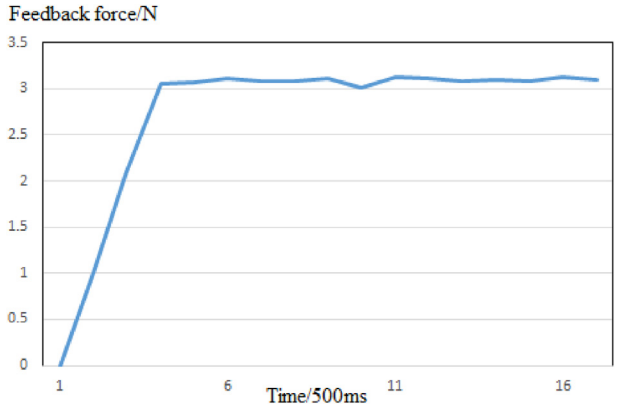

Fig. 15. The measured operating resistance by using the instrument with different setting of force model variables.

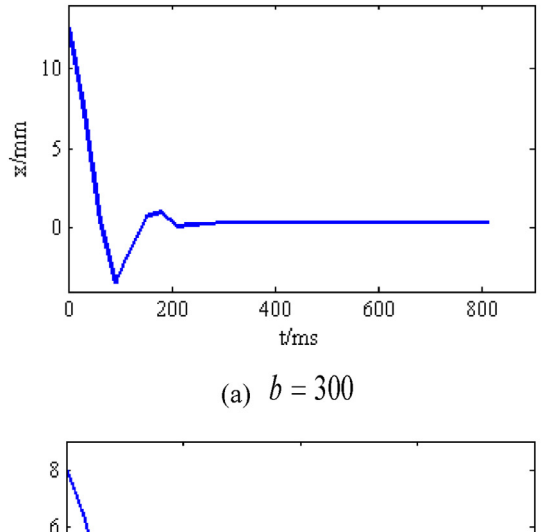

(a) $b = 300$

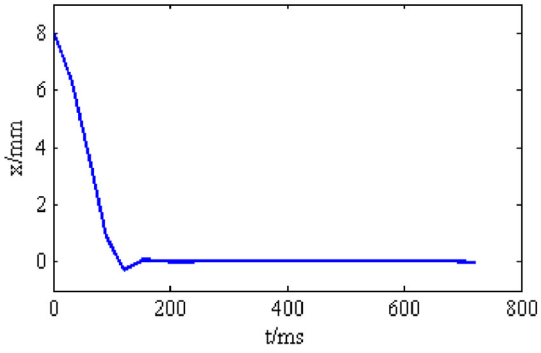

(b) $b = 400$

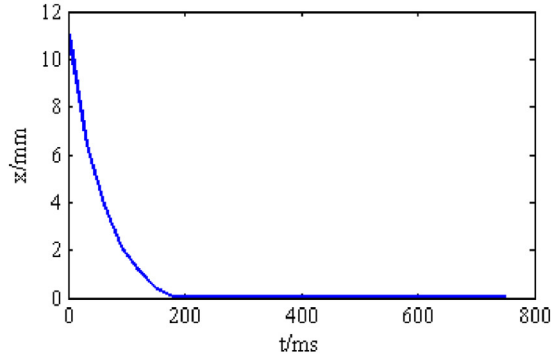

(c) $b = 500$

Fig. 16. The relationship between the effectiveness of home function and the damping coefficient of spring-damping model used in feedback force computation.

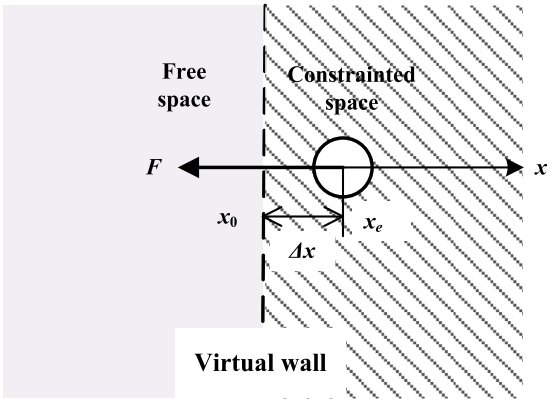

Fig. 17. The diagram to depict the force model and haptic rendering of virtual wall.

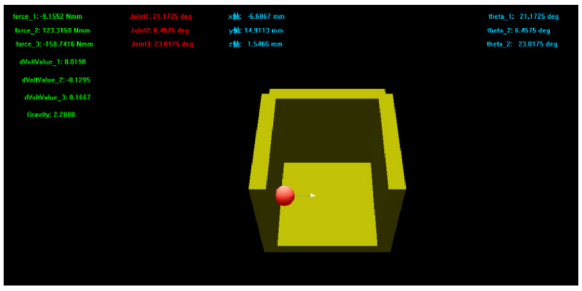

Fig. 18. The virtual wall to test the DELTA mechanism based haptic device by using the conventional spring-damping model, and the simulated contact force is computed based on the same spring-damping model used to render operating resistance.

Table 13
The measured maximum output stiffness along three axes.

x	y	z
4.9 N/mm	5.1 N/mm	4.5 N/mm

any position in the workspace. Therefore, the home function is also testified to determine the optimal value of the damping coefficient. In the spring-damping model, the weight of damping force is used to keep the haptic loop stable. From Fig. 16 (a, b, c), *b* (N.s/m) is the damping coefficient, the results illustrate that larger damping coefficient can avoid oscillation and decrease error of the home function. For the designed haptic device, the damping coefficient is set to be 500 N·s/m.

5.3. Virtual wall

Virtual wall is usually utilized to demonstrate the performance of a haptic device, which uses the spring-damping model to render contact force between the tool and the wall in a virtual environment. Fig. 17 and Eq. (24) depict the haptic rendering algorithm of virtual wall. From Fig. 17, a user feels no feedback force when he manipulates the device to move the virtual ball in the free space. However, when he manipulates the designed haptic device to move the virtual ball to touch the virtual wall and enter the constrained space from the free space, he will feel resistance rendered by using Eq. (24). Fig. 18 shows the virtual environment.

$$\mathbf{F} = \begin{cases} K_e(\mathbf{x_e} - \mathbf{x_0}) & |\mathbf{x_e}| > |\mathbf{x_0}| \\ 0 & |\mathbf{x_e}| < |\mathbf{x_0}| \end{cases} \tag{24}$$

Where, **F** is the feedback force, and K_e is the spring stiffness. At first, the value of spring stiffness is set 1.1 N/mm and increased per 0.2 N/mm. During the whole experiment, users should feel smooth feedback force without any oscillation or instability. Table 13 depicts the measured maximum simulated stiffness along the three axes, which illustrates that the DELTA mechanism optimized by using the proposed GA/SQP methodology works well.

6. Conclusions

This paper describes GA and SQP optimization for the design of a DELTA configuration based haptic device. The optimization results of GA and SQP are compared and discussed. Using the result of GA as the start point of SQP is testified to be a useful and efficient way to find the optimal solution.

Based on the optimization methodology, the optimal dimensions of the DELTA mechanism can be identified to perform well in haptic display, and the largest cube workspace can be obtained while all the constraints are satisfied. The condition number of the Jacobian matrix is used to evaluate the performance of the DELTA mechanism in haptic display. The smallest value of the maximum condition number of Jacobian matrix at all the points of the cube workspace is chosen as the final objective of optimization.

A haptic joystick has been designed by using the proposed method to demonstrate all the optimal values of the four design variables. The proposed method is simple and is shown to be effective in finding the optimal dimensions of the DELTA mechanism having the best achievable specification as a haptic joystick for the given constraints. Now, this optimization scheme is being developed to implement dimensional synthesis of a six DOF parallel mechanism based haptic device design.

Acknowledgment

This research was supported by China Domestic Research projects under grants 2012GB102006 and 2012GB102008

References

[1] R. Clavel, Une nouvelle structure de manipulation paralle ‘le pour la robotique le ´ge ‘re, R.A.I.R.O, APII 23 (6) (1986).
[2] M. Stock, K. Miller, Optimal kinematic design of spatial parallel manipulators: application to linear delta robot, J. Mech. Design 125 (2) (2003) 292–301.
[3] Peter Vischer, Clavel, et al., Kinematic calibration of the parallel delta robot, Robotica 16 (2) (1998) 207–218.
[4] B. Zi, J. Lin, S. Qian, Localization, obstacle avoidance planning and control of a cooperative cable parallel robot for multiple mobile cranes, Rob. Comput.-Integr. Manuf. 34 (2015) 105–123.
[5] J. Mo, Z.F. Shao, L. Guan, et al., Dynamic performance analysis of the X4 high-speed pick-and-place parallel robot, Rob. Comput.-Integr. Manuf. 46 (C) (2017) 48–57.
[6] Grange S. Delta haptic device as a nanomanipulator. 2001, 4568 (1):100–111.
[7] E. Ottaviano, C.M. Gosselin, M. Ceccarelli, Singularity analysis of capaman: a three--degree of freedom spatial parallel manipulator, in: IEEE international conference on robotics and automation, 2001. Proceedings, 2, IEEE, 2001, pp. 1295–1300.
[8] G.L. Long, C.L. Collins, A pantograph linkage parallel platform master hand controller for force-reflection, in: IEEE International Conference on Robotics and Automation, 1992. Proceedings, 1, IEEE, 1992, pp. 390–395.
[9] H. Noma, H. Iwata, Presentation of multiple dimensional data by 6 DOF force display, in: Ieee/rsj International Conference on Intelligent Robots and Systems ’93, IROS, 3, IEEE, 1993, pp. 1495–1500.
[10] Y. Tsumaki, H. Naruse, D.N. Nenchev, et al., Design of a compact 6-DOF haptic interface, in: IEEE International Conference on Robotics and Automation, 1998. Proceedings, 3, IEEE, 1998, pp. 2580–2585.
[11] L.W. Tsai, Robot Analysis and Design: The Mechanics of Serial and Parallel Manipulators, John Wiley & Sons, Inc, 1999.
[12] R. Boudreau, C.M. Gosselin, The synthesis of planar parallel manipulators with a genetic algorithm, ASME J. Mech. Design 121 (1999) 533–537.
[13] R. Boudreau, C.M. Gosselin, La synthèse d’une plate-forme de Gough-Stewart pour un espace atteignable prescrit, Mech. Mach. Theory 36 (3) (2001) 327–342.
[14] A. Kosinska, M. Galicki, K. Kedzior, Designing and optimization of parameters of delta-4 parallel manipulator for a given workspace, J. Rob. Syst. 20 (9) (2003) 539–548.
[15] A.M. Hay, J.A. Snyman, Optimal synthesis for a continuous prescribed dexterity interval of a 3-dof parallel planar manipulator for different prescribed output workspaces, Int. J. Numer. Methods Eng. 68 (1) (2010) 1–12.
[16] M.A. Laribi, A. Mlika, L. Romdhane, et al., A combined genetic algorithm–fuzzy logic method (GA–FL) in mechanisms synthesis, Mech. Mach. Theory 39 (7) (2004) 717–735.
[17] L. Romdhane, Design and analysis of a hybrid serial-parallel manipulator, Mech. Mach. Theory 34 (7) (1999) 1037–1055.
[18] M. Gallant, R. Boudreau, The synthesis of planar parallel manipulators with prismatic joints for an optimal singularity-free workspace, J. Robot. Syst. 19 (1) (2002) 13–24.

[19] B. Zi, H. Sun, D. Zhang, Design, analysis and control of a winding hybrid-driven cable parallel manipulator, Rob. Comput.-Integr. Manuf. 48 (2017) 196–208.
[20] B. Zi, H. Ding, J. Cao, et al., Integrated mechanism design and control for completely restrained hybrid-driven based cable parallel manipulators, J. Intell. Rob. Syst. 74 (3-4) (2014) 643–661.
[21] J.E. Colgate, J.M. Brown, Factors affecting the Z-Width of a haptic display, in: IEEE International Conference on Robotics and Automation, 1994. Proceedings, 4, IEEE, 1994, pp. 3205–3210.
[22] J. An, D.S. Kwon, In haptics, the influence of the controllable physical damping on stability and performance, in: Ieee/rsj International Conference on Intelligent Robots and Systems, 2, IEEE, 2005, pp. 1204–1209.
[23] J.J. Gil, M.J. Puerto, I. Díaz, et al., On the Z-width limitation due to the vibration modes of haptic interfaces, in: Ieee/rsj International Conference on Intelligent Robots and Systems, IEEE, 2010, pp. 5054–5059.
[24] N. Yasrebi, D. Constantinescu, Extending the Z-width of a haptic device using acceleration feedback, in: International Conference on Haptics: Perception, Devices and Scenarios, Springer-Verlag, 2008, pp. 157–162.
[25] Y. Lou, Y. Zhang, R. Huang, et al., Optimization algorithms for kinematically optimal design of parallel manipulators, IEEE Trans. Autom. Sci. Eng. 11 (2) (2014) 574–584.
[26] M. Antonio, E.J. Solteiro, R. Manuel, Design of a parallel robotic manipulator using evolutionary computing, Int. J. Advanced Rob. Syst. 9 (1-2) (2012) 1.
[27] A. Ghosal, B. Ravani, A differential-geometric analysis of singularities of point trajectories of serial and parallel manipulators, J. Mech. Design 123 (1) (2001) 80–89.
[28] G. Liu, Y. Zhang, D. Wang, et al., Stable haptic interaction using a damping model to implement a realistic tooth-cutting simulation for dental training, Virtual Reality 12 (2) (2008) 99–106.